Research Article J. Electrochem. Sci. Technol., 2019, 10(2), 244-249

Multidimensional Conducting Agents for a High-Energy-Density Anode with SiO for Lithium-Ion Batteries

Suhyun Lee[1], Nakgyu Go[1], Ji Heon Ryu[2], and Junyoung Mun[1,*]

[1]Department of Energy and Chemical Engineering, Incheon National University, 12-1, Songdo-dong, Yeonsu-gu, Incheon 22012, Republic of Korea

[2]Graduate School of Knowledge-based Technology, Korea Polytechnic University, Siheung-si, Gyonggi-do, Republic of Korea

ABSTRACT

SiO has a high theoretical capacity as a promising anode material candidate for high-energy-density Li-ion batteries. However, its practical application is still not widely used because of the large volume change that occurs during cycling. In this report, an active material containing a mixture of SiO and graphite was used to improve the insufficient energy density of the conventional anode with the support of multidimensional conducting agents. To relieve the isolation of the active materials from volume changes of SiO/graphite electrode, two types of conducting agents, namely, 1-dimensional VGCF and 0-dimensional Super-P, were introduced. The combination of VGCF and Super-P conducting agents efficiently maintained electrical pathways among particles in the electrode during cycling. We found that the electrochemical performances of cycleability and rate capability were greatly improved by employing the conducting agent combinations of VGCF and Super-P compared with the electrode using only single VGCF or single Super-P. We investigated the detailed failure mechanisms by using systematic electrochemical analyses.

Keywords : High Capacity Anode, SiO/graphite, Conducting Agent, VGCF, Super-P

Received : 20 December 2018, Accepted : 26 February 2019

1. Introduction

Fine dust pollution and diesel gate are highlighting the importance of eco-friendly vehicles, i.e., electric vehicles (EVs) [1-3]. The insufficient performance of lithium-ion batteries (LIBs) critically limits the affordability of the EVs. To extend the efficiency for the EVs for widespread use in our daily lives, it is essential to improve the energy density of the LIBs. At the same time, the importance of energy storage systems (ESSs) has been emphasized due to the fluctuating renewable energy resources that are required to be load leveling. Since the scale of LIBs for the ESSs is more than 100 times the capacity for EV batteries, the high energy density of LIBs considerably reduce the cost and space burden for the large scale use of LIBs in ESSs. These very large systems require a large scale of LIBs from kWh to MWh, which is much larger than that for small portable electronic devices. For affordable large scale LIBs, it is necessary to improve the energy density of the LIBs. Accordingly, many researchers in the LIB community are studying high-energy-density active materials [4,5]. Whereas graphite, which is the most typical anode material for conventional LIBs, does not have a sufficient theoretical capacity, 372 mAh g^{-1}, silicon (Si) has a high theoretical capacity of 4400 mAh g^{-1} [6-10]. Even with this distinct advantage of Si, it has problems for practical applications as an anode material for commercialized LIBs. During Li insertion/extraction in Si, very large volume changes lead to pulverizing of the electrode, causing detrimental cycle life [6,10-15].

Many researchers have investigated the optimal approaches between energy density and cycleability by introducing a buffer matrix for relieving volume changes and maintaining the electrode matrix [16-18]. Si, having various types of inert matrixes, such as metal, carbon and inorganic components, exhib-

*E-mail address: jymun@inu.ac.kr

DOI: https://doi.org/10.5229/JECST.2019.10.2.244

ited improved cycleability but reduced capacity. The high capacity of Si enables this approach because the reduced capacity caused by introducing the buffer matrix is usually higher than that of graphite. Among these concepts, SiO-based materials have also attracted much attention as a promising anode material because SiO generates a buffer component SiO_2 [19-22]. Additionally, its preparation is very affordable. Despite the fact that it has a smaller theoretical capacity than pure Si active material, cycle performance can be highly improved to close to commercialization. However, it still has a large volume change and cannot totally solve the abovementioned problems caused by pulverization. New concepts are required to solve these critical problems of poor electronic conductivity and pulverization. Therefore, many researchers have focused on improving the electrochemical performances of SiO-based anode materials [19-21,23,24].

In this work, we tried to improve the electrochemical performances of SiO/C composite electrodes by using various conducting agents having different morphologies, VGCF and Super-P. The optimal combination of VGCF and Super-P for SiO/C electrode was investigated to relieve the failure mechanism of high capacity anode material. To elucidate the detail mechanisms, the surface analyses and the electrochemical experiments were performed. Electrochemical behaviors of half-cells were evaluated with four kinds of electrodes by controlling the ratios between VGCF and Super-P.

2. Experimental

Electrode preparation - SiO/graphite electrodes were prepared by coating an aqueous solution-based slurry consisting of 94 wt% active materials (SiO and graphite = 10:90 wt%), 3 wt% conducting agents, and 3 wt% binder (SBR/CMC = 2:1) onto copper foil. The total concentration of conducting agents was fixed at 3 wt%; the VGCF/Super-P conducting agents were portioned out in the ratios of 0:3, 1:2, 2:1 and 0:3. The electrode sheet on which the slurry was cast was thoroughly dried in a convection oven at a temperature of 80°C. The electrode was then pressed using a roll presser.

Characterization - The surface morphologies of these electrodes were observed using field emission scanning electron microscopy (FE-SEM, JSM-7001F). The electronic conductivities of the mixture of conducting agent and active materials were measured using a four-probe method under various pressures of 200, 400 and 600 kgf.

Electrochemical Characterization - Each electrode sheet was punched into a disk shape of diameter of 1.2 cm. The composite electrodes were thoroughly dried at 120°C in a vacuum oven overnight, and 2032-type coin half cells were fabricated in an Ar-filled glove box. The coin-type half cells consisted of Li metal foil as the counter electrode and a polypropylene separator (Celgard) with electrolyte (1.0 M $LiPF_6$ / EC:DEC (3:7 vol%), Panaxetec). After assembly, the coin cells were at rest for 12 hours before the electrochemical measurements. The electrochemical performance of the cells was evaluated using a Wonatech WBCS 3000. For the first cycle (as a formation cycle), they were first charged under 0.05 C (lithiation, 1 C = 450 mA g^{-1}) and discharged (de-lithiation) under 0.1 C of the current density in the potential range of 0.005 to 2.0 V in the chamber at room temperature. After the initial cycle, the second and third cycles were charged and discharged under the same current density of 0.1 C. Then, the subsequent cycles were charged at 0.2 C and discharged at 0.5 C. Galvanostatic intermittent titration technique (GITT) measurements were performed using WBCS-3000 cyclers (Wonatech). After charging with a current density of 0.05 C for 50 mAh g^{-1}, the cell potential was stabilized to OCV by using a rest step for an hour. The same process was repeated until the accumulated charging capacities reached 500 mAh g^{-1}. The discharge sequence was followed by using 0.5 C current density until the potential reached 2.0 V under the same capacity condition.

3. Results and Discussion

Fig. 1 depicts the SEM images of the electrodes comprising SiO and graphite with various combinations of VGCF and Super-P conducting agents. Two types of active materials can be clearly distinguished by different contrast in all SEM images due to different electronic conductivities between SiO and graphite. The bright particles are thought to be SiO because emitting electrons are stacked on the surface due to the poor conductivity of SiO. In contrast, the dark particles are graphite, which has high conductivity. The SEM images from the electrode having VGCF

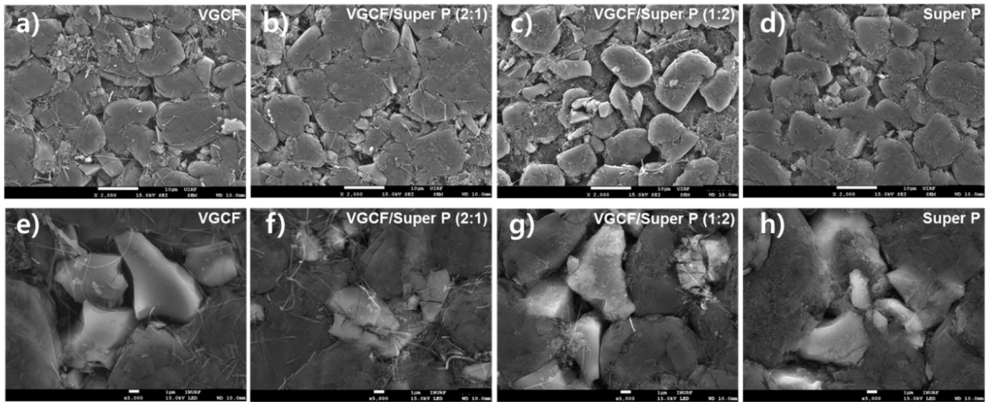

Fig. 1. FE-SEM images from the pristine composite electrodes with a) VGCF, b) VGCF/Super-P (2:1), c) VGCF/Super-P (1:2), and d) Super-P. e), f), g), h) The magnified SEM images of the VGCF, VGCF/Super-P (2:1), VGCF/Super-P (1:2) and Super-P electrodes.

exhibit a distributed wire-type VGCF (Figs. 1a-c). Additionally, the electrodes with the combination of VGCF and Super-P also have nanosize round carbon particles that are Super-P (Fig. 1b and c). It is noted that the electrode with the single conducting agent of VGCF, Fig. 1a, has certain spaces in which carbon conducting agents are not filled. In contrast, an amount of carbon is homogeneously distributed in the electrode with Super-P (Fig. 1d). Basically, VGCF and Super-P are uniformly mixed in the electrodes (Figs. 1c and d). The enlarged images have similar tendencies from Fig. 1e to 1h.

The electronic conductivities of the pellets with conducting agent and active material of SiO and graphite were evaluated under various pressures from 200 to 400 kgf and the results are shown in Fig. 2. As the pressure increases, the conductivity also increases because high pressure leads to efficient electron pathways by reducing voids between the particles. The conductivities of the pellet with only VGCF are 20, 37 and 55 under various pressures of 200, 400 and 600 loads, respectively. Under the same conditions, the pellet with the single conducting agent of Super-P sample presents conductivities of 23, 40, and 58, respectively, which are higher than the conductivity of the VGCF sample. Even though the electronic conductivity of VGCF having high crystallinity is higher than Super-P, the electrode having only VGCF was not better than the electrode with Super-P. As shown in Fig. 1a, the electrode having VGCF contains voids between the particles, which highly limit the electron pathway. Based on the similar FE-SEM images, the sample with pure Super-P also has a similar level of conductivity to the VGCF sample. The electrode having two types of conducting agent exhibited higher conductivity than the electrode with only a single type of conducting agent. It is thought that the distribution of the conducting agent as well as its electronic conductivity is also important.

The electrochemical behaviors of the electrodes with different conducting agents were further evaluated by GITT upon first cycle (Fig. 3). In order to equally control the volume expansion by the same amount of lithiation, the specific charge capacity was accurately controlled to 500 mAh g^{-1} by a low current density of 22.5 mA g^{-1} (0.05 C). It is found that the green curve from the electrode having only Super-P always has a lower potential for the lithiation curve than the others, representing a high resistance. However, different discharge capacities were obtained from the experimented cells. A large volume change accelerated the pulverization of the electrode, but the 1D conducting agent of VGCF reduced the failure mode from particle isolation via electronically linking the particles over the space. The difference in discharge capacities from the cells also reflect different electrochemical behavior during the lithiation process. As shown at the end of discharge at the accumulated specific capacity of 850 mAh g^{-1} in Fig. 3, the cell with Super-P (green curve) exhibits the voltage curve at the highest position. This means that the round-type conducting agent is not sufficient to hold

the electron path long after the volume changes during lithiation, whereas the combination of VGCF and Super-P (red curve) has a higher capacity and lower potential throughout the discharge sequence. This indicates that the combination works well in reducing resistance and reversibility.

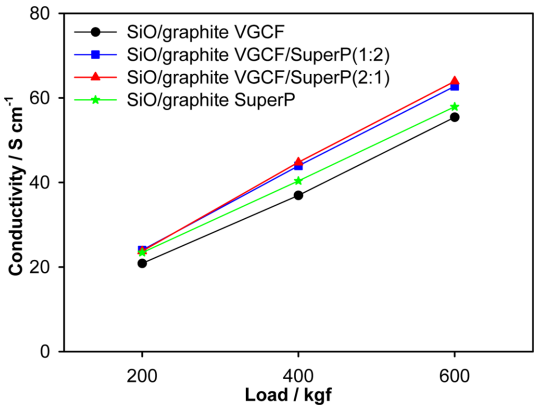

Fig. 2. Electronic conductivities from pellets having SiO, graphite and conducting agents by a 4-probe method under various pressures from 200 to 600 kgf cm^{-2}.

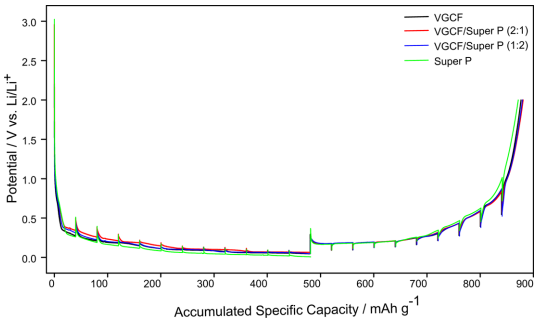

Fig. 3. GITT voltage curves from the cells having various conducting agents.

Fig. 4a presents the first voltage profiles of the electrodes with the different conducting agents VGCF and Super-P in different ratios. For this figure, the potential range from 2 and 0.01 V were used. In Fig. 4a, the initial discharge capacities of the cells are similar to each other and the initial coulombic efficiencies are calculated to be above 8d5 % in all samples (86.7, 86.2, 87.9, and 86.6 % for VGCF3:SP0, VGCF2:SP1, VGCF1:SP2, and SP3, respectively). Those cells exhibited different charging capacities of 576.7, 596.3, 600.6, and 598.9 mAh g^{-1} for VGCF3:SP0, VGCF2:SP1, VGCF1:SP2, and SP3, respectively. The anode having Si based material has the largest volume change at the end of charge, so the reversibility of the end of charge sequence is efficient to understand the role of conducting agents in this paper. Therefore, to distinguish the detrimental effect in the end of charging process, we tried to use different volumes changes by various charging conditions. A new group was added, in which the initial charging capacities were controlled to 450 mAh g^{-1} (Fig. 4b). In Fig. 4b, it is confirmed that the initial coulombic efficiencies are 84.4, 83.4, 83.5 and 82.8% for VGCF3:SP0, VGCF2:SP1, VGCF1:SP2, and SP3, respectively. As the portion of the initial electrolyte decomposition in the charging capacity increase, the coulombic efficiencies decrease. In Fig. 4b, under the same charging capacity condition, the irreversible capacity of the cell having the Super-P electrode was higher than the other types of electrodes having VGCF as single or combination conducting agents. Fig. 4c shows the coulombic efficiencies under the charged capacity (450 mAh g^{-1}). The error bar was obtained by compared fig. a and Fig. 4b, the electrode using combined conducting agents has higher coulombic efficiency than single Super-P and single VGCF. Si particles have a large volume change

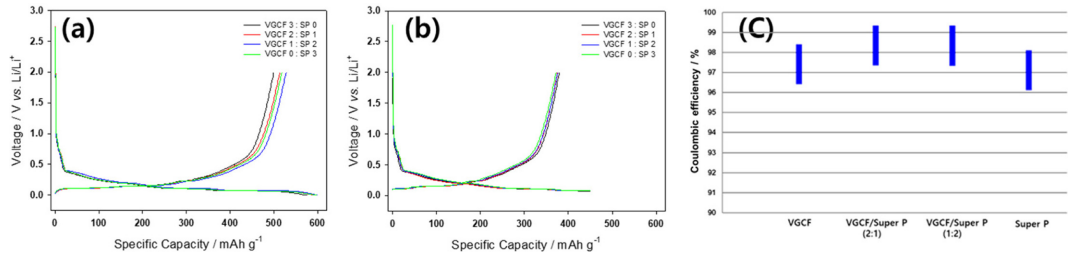

Fig. 4. the 1st voltage curves a) in the potential range from 5 mV to 2 V and b) with the limitation of 450 mAh g^{-1}·c) Coulombic efficiencies by using a higher charge capacity than 450 mAh g^{-1} by combination with a) and b).

during Li insertion/extraction in Si. Thus, the Si particle of single Super-P used sample was separated from other Si particles and conducting agent. Therefore, the Si particles isolated by the volume change were not connected to the electron transfer pathway. However, the mixed VGCF and Super-P conducting agent samples kept conducting long after the volume change, because VGCF is connected to the Si particles to keep conducting long after the volume change.

Fig. 5 presents the cycling performance of cells having different morphologies of conducting agents. During the initial 20 cycles, the capacity decreases were prominent due to large volume changes. After decreasing the capacity, the cycleability was stabilized because of low volume changes. In this trend, the electrode having VGCF/Super-P (2:1) exhibited better cycleability than the others. The specific capacity of VGCF / Super-P (2: 1) sample was 403 mAh g^{-1} after 40 cycles, indicating a capacity higher than 370 mAh g^{-1} of graphite.

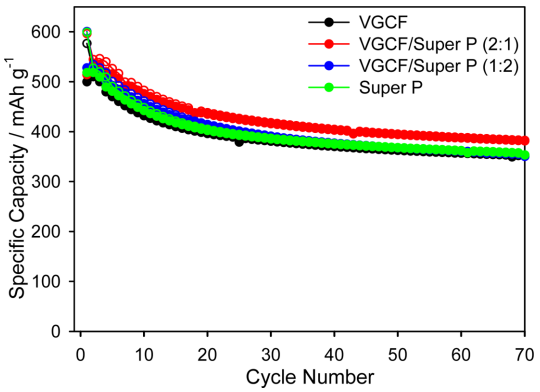

Fig. 5. Cycleability with the cells having VGCF, VGCF/Super-P (2:1), VGCF/Super-P (1:2), and Super-P. The current density was 0.5 C for discharge and 0.2 C for charge (1C = 450 mA g^{-1}). Filled and blank circles represent for discharge and charge capacity, respectively.

To check the power density, the rate capability with various discharging current conditions was studied. Fig. 6 exhibits rate capabilities of cells having various ratios of VGCF and Super-P. The rate capability was performed under different current densities of 1 C, 3 C, 5 C, 10 C, and 15 C. Being similar with the cycleability, the VGCF / Super-P (2:1) sample also maintained a higher specific discharge capacity at various current densities than the other electrodes.

4. Conclusions

The optimal combination and the effect of multidimensional conducting agents of VGCF and Super-P for SiO/C electrode were investigated to relieve the failure mechanism of the high-capacity anode material having large volume changes. To elucidate the mechanisms, surface analyses and electrochemical experiments were performed. The multishaped conducting agent with VGCF can maintain electrical connectivity to avoid isolation of SiO particles. However, the high density and 1-dimensional VGCF caused a void space among particles, in turn causing high polarizations by reducing distribution of the conducting agent. However, the combination of VGCF and Super-P for the SiO/C electrode gave stable cycle performance. It was also confirmed that reversibility of the capacity was better in the electrodes using the combined conducting agents of VGCF and Super-P than in the electrodes using single VGCF or single Super-P.

Acknowledgment

This work was supported by the Incheon National University (International Cooperative) Research grant in 2015.

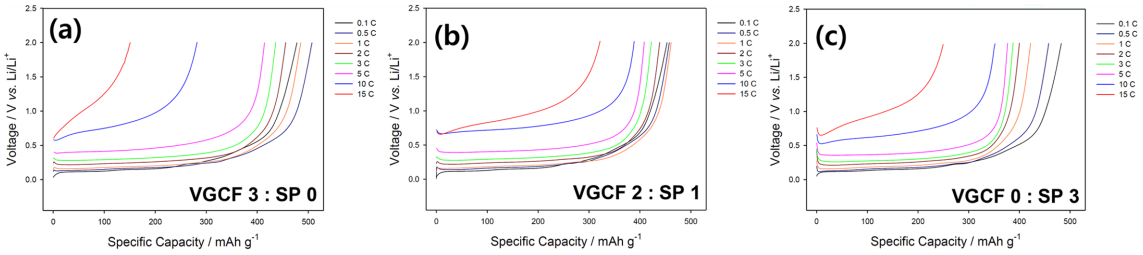

Fig. 6. Discharge voltage curve from cells having various conducting agent systems: a) VGCF, b) VGCF:Super-P (2:1), c) Super-P.

References

[1] H.H. Sun, A. Manthiram, *Chem. Mat.*, **2017**, *29(19),* 8486-8493.

[2] S.H. Jang, J. Mun, D.-K. Kang, T. Yim, *J. Electrochem. Sci. Technol.*, **2017**, *8(2),* 162-168.

[3] A. Riaz, K.N. Jung, J.W. Lee, *J. Electrochem. Sci. Technol.*, **2015**, *6(2),* 50-58.

[4] A. Tron, H. Kang, J. Kim, J. Mun, *J. Electrochem. Sci. Technol.*, **2018**, *9(1),* 60-68.

[5] A. Tron, T. Yoon, Y.D. Park, S.M. Oh, J. Mun, *J. Nanosci. Nanotechnol.*, **2017**, *17(7),* 4977-4982.

[6] S. Lim, H. Chu, K. Lee, T. Yim, Y.-J. Kim, J. Mun, T.-H. Kim, *ACS Appl. Mater. Interfaces*, **2015**, *7(42),* 23545-23553.

[7] S.J. Choi, T. Yim, W. Cho, J. Mun, Y.N. Jo, K.J. Kim, G. Jeong, T.-H. Kim, Y.-J. Kim, *ACS. Sustain. Chem. Eng.*, **2016**, *4(12)*, 6362-6370.

[8] S. Lim, K. Lee, I. Shin, A. Tron, J. Mun, T. Yim, T.-H. Kim, *J. Power Sources*, **2017**, *360,* 585-592.

[9] K. Lee, S. Lim, A. Tron, J. Mun, Y.-J. Kim, T. Yim, T.-H. Kim, *RSC Adv.*, **2016**, *6(103),* 101622-101625.

[10] M. Zhang, T. Zhang, Y. Ma, Y. Chen, *Energy Storage Mater.*, **2016**, *4,* 1-14.

[11] H. Wu, G. Chan, J.W. Choi, I. Ryu, Y. Yao, M.T. McDowell, S.W. Lee, A. Jackson, Y. Yang, L. Hu, Y. Cui, *Nat Nano*, **2012**, *7(5),* 310-315.

[12] N. Dimov, S. Kugino, M. Yoshio, *Electrochim. Acta*, **2003**, *48(11),* 1579-1587.

[13] S.D. Beattie, M.J. Loveridge, M.J. Lain, S. Ferrari, B.J. Polzin, R. Bhagat, R. Dashwood, *J. Power Sources*, **2016**, *302,* 426-430.

[14] R. Zhou, R. Fan, Z. Tian, Y. Zhou, H. Guo, L. Kou, D. Zhang, *J. Alloys Compd.*, **2016**, *658,* 91-97.

[15] B.-C. Yu, Y. Hwa, J.-H. Kim, H.-J. Sohn, *J. Power Sources*, **2014**, *260,* 174-179.

[16] J. Yang, Y. Wang, W. Li, L. Wang, Y. Fan, W. Jiang, W. Luo, Y. Wang, B. Kong, C. Selomulya, H.K. Liu, S.X. Dou, D. Zhao, *Adv. Mater.*, **2017**, *29(48)*, 1700523.

[17] X. Fan, J. Ji, X. Jiang, W. Wang, Z. Liu, *RSC Adv.*, **2016**, *6(82),* 78559-78563.

[18] T. Kim, Y.H. Mo, K.S. Nahm, S.M. Oh, *J. Power Sources*, **2006**, *162(2),* 1275-1281.

[19] T. Xu, J. Zhang, C. Yang, H. Luo, B. Xia, X. Xie, *J. Alloys Compd.*, **2018**, *738,* 323-330.

[20] L. Guo, H. He, Y. Ren, C. Wang, M. Li, *Chem. Eng. J.*, **2018**, *335,* 32-40.

[21] J. Zhang, J. Gu, H. He, M. Li, *J. Solid State Electrochem.*, **2017**, *21(8),* 2259-2267.

[22] L. Wu, H. Zhou, J. Yang, X. Zhou, Y. Ren, Y. Nie, S. Chen, *J. Alloys Compd.*, **2017**, *716,* 204-209.

[23] Z. Li, Q. He, L. He, P. Hu, W. Li, H. Yan, X. Peng, C. Huang, L. Mai, *J. Mater. Chem. A*, **2017**, *5(8),* 4183-4189.

[24] K. Kim, H. Choi, J.H. Kim, *Appl. Surf. Sci.*, **2017**, *416,* 527-535.